



INFLUENCE OF BUILDING HEIGHT AND GROUND MOTION TYPE ON THE SEISMIC BEHAVIOUR OF ZIPPER CONCENTRICALLY BRACED STEEL FRAMES

Tirca, L.¹ and Tremblay, R.²

SUMMARY

This paper presents an analytical study of the response of 4-, 8-, and 12-storey concentrically braced steel frames with zipper columns under three different seismic ground motions: regular crustal earthquakes, near field earthquakes and long duration subduction earthquakes. A design procedure proposed to ensure elastic zipper column response was found adequate for most cases but tension forces exceeding the predicted loads developed in the lower floors of the 8- and 12-storey buildings. The performance of all structures was satisfactory under the regular motions. Collapse by dynamic instability occurred for the 8- and 12-storey structures under near field and subduction earthquakes.

INTRODUCTION

In view of their simplicity and high efficiency in resisting lateral loads, chevron, or inverted V-braced frames are among the most popular configurations adopted for concentrically braced steel structures in Canada. Past studies (Khatib et al. [1]; Tremblay and Robert [2]) have shown, however, that this system is prone to storey mechanisms under seismic ground motions, with excessive storey drifts and large brace ductility demand developing in compression. Variations in storey shear capacity and degradation of the brace compression strength after brace buckling tend to concentrate earthquake damage in a few stories. In particular, the unbalanced vertical loads imposed on beams after brace buckling induce plastic hinging in the beams, preventing the development of the brace tension capacity and leading to reduced storey shear resistance. Due to the limited ability of chevron bracing to redistribute the inelastic demand over the structure height, the system is sensitive to dynamic instability under seismic motions. Building height limitations and minimum lateral resistance requirements have been introduced in CSA S16-01 Standard [3] to mitigate this problem. Alternatively, the beams can be designed to resist forces imposed after buckling of the braces, which enhances the overall response and allows taller frames and reduced design seismic loads to be used. This approach has been studied by several researchers (Remennikov and Walpole [4]; Khatib et al.; Sabelli [5]; Tremblay and Robert) and has been introduced in design codes [3,

¹Design Engineer, Canam Manac Group, Boucherville, Canada

²Professor, Dept. of Civil, Geological and Mining Engineering, Ecole Polytechnique of Montreal, Montreal Canada H3C 3A7 Email : tremblay@struc.polymtl.ca

6, 7]. However, this design strategy requires a significant amount of additional steel and the soft-storey mechanisms still remains possible.

In order to limit further the risk of soft-storey response, Khatib et al. proposed to add zipper columns in chevron bracing, linking together all brace-to-beam intersecting points to force the formation of a complete plastic mechanism involving buckling of the braces over the entire building height (see Fig. 1). For such a structural configuration, it was anticipated that the response would not be sensitive to ground motion signatures, implying that the structure inelastic behavior will not vary much from one earthquake record to another. For this system, it is desirable that zipper columns be designed to remain essentially elastic under strong ground motions effects, without buckling or yielding as shown in Fig 1. Khatib et al. proposed to determine the axial tension load in the zipper column through an SSRS combination of the vertical components of the unbalanced brace loads at every floor, whereas design compression loads were limited by the flexural capacity of the beams. Good correlation was obtained for a 6-storey structure between zipper column forces so predicted and the values obtained from nonlinear dynamic analysis, although considerable scatter in peak zipper column forces was observed under different ground motions.

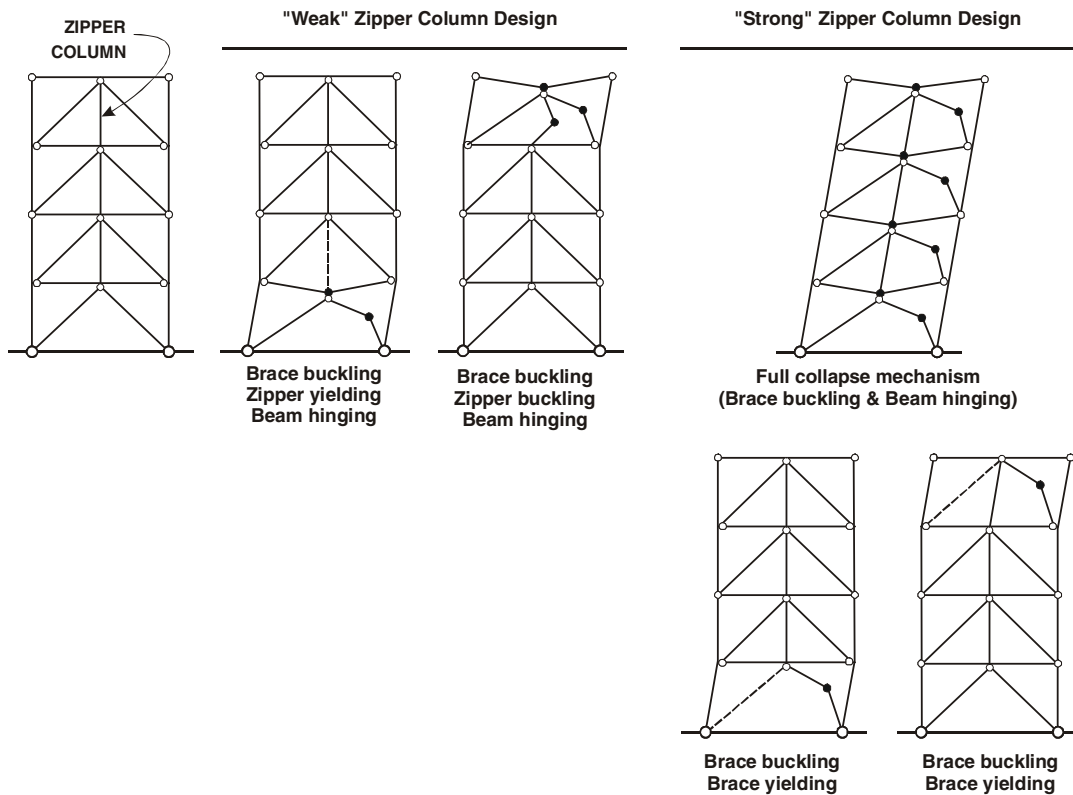


Figure 1: Anticipated collapse mechanisms for CBF systems with weak and strong zipper columns.

Sabelli studied a 3- and a 6-storey zipper braced frames in which the zipper columns were given the same section as the braces at the same level. The inelastic demand on the braces was found to be much more uniform than that obtained in reference chevron bracing designed with strong beams. The behavior of the 6-storey zipper frame was also influenced by second mode response. The author recommended that zipper columns possess the same compression and tension strengths as the braces located at the level below and the column be detailed with the expectation of inelastic demand. Tremblay and Tirca [8] proposed a method to predict zipper column loads in which different scenarios of brace buckling sequences and

subsequent force redistribution are considered. The method was found to result in conservative estimates for zipper compression loads and accurate prediction for the tension loads for an 8-storey structure subjected to ordinary ground motions as well as near field records. The compression loads obtained from analysis exceeded significantly, however, the values predicted using the method proposed by Khatib. A study by Tremblay [9] showed, however, that elastic response of the zipper columns does not guarantee good overall performance and dynamic stability under strong ground motions as the structure response still heavily relies on the hysteretic behavior of steel bracing members, which is far from ideal due to the degradation of the brace compressive strength, pinching, and accumulated permanent elongation of the braces. Figure 2 shows global and local collapse mechanisms for braced frames with strong zipper columns for which the capacity is governed by the post-buckling strength of the braces.

This paper presents an analytical study that was performed to examine further the influence of the building height and the signature of ground motions on the seismic performance of zipper concentrically braced steel frames. The study included 4-, 8-, and 12-storey building structures subjected to three different ground motion ensembles: ordinary ground motions from crustal and sub-crustal events, records from near field earthquakes, and long duration ground motions produced by subduction events. The structures were designed according to Canadian seismic design provisions and the zipper columns were sized according to the method proposed by Tremblay and Tirca. The objectives of the study were to validate the adequacy of that method and verify the seismic performance of the structures for the various building geometries and ground motion types. The first part of the building briefly summarizes the design procedure for the zipper column. The seismic design and performance of the sample structures are respectively presented in the second and third parts of the paper.

DESIGN METHODOLOGY FOR ZIPPER FRAMES

In the design procedure, the braces are the first elements to be designed and this is done according to normal concentrically braced frame design practice, i.e. using member forces obtained from elastic analysis of the structure under code specified load combinations and applying seismic detailing provisions for ductile inelastic cyclic brace response. Beams must be continuous over their entire length and compact cross sections must be selected as plastic hinging is anticipated at beam mid-span. Edge columns of the bracing bents are designed to carry the compression load resulting from the tributary gravity loads acting together with the action of the braces reaching simultaneously their expected compressive strength, C_u , at all levels.

Compression forces in the zipper columns result from buckling of the braces in the upper levels whereas tension forces are induced after brace buckling has occurred at the lower floors. Therefore, these two conditions must be considered to predict adequately both axial loads. In addition, various scenarios must be studied to capture the possible sequences of brace buckling in the lower and upper parts of the frame. For compression, the most critical and likely situation is when brace buckling starts at the top of the structure and propagates towards the base of the frame. Similarly, tension forces in zipper columns should be evaluated when brace buckling initiates at the base and progresses up in the frame.

In the proposed method, the compression forces acting in the zipper columns are determined for (n-1) different scenarios, where n is the number of stories. As shown in Fig. 2a, in each scenario, braces are assumed to have buckled at a given floor and at all the floors above, while the compression brace at the floor below is near buckling or has just buckled and can still develop its full compression resistance, C_u . Buckled braces are assumed to impose an axial compression force equal to their post-buckling strength, C'_u . The first scenario involves buckling of the brace at the uppermost level and brace buckling propagates towards the base in the subsequent scenarios. For each scenario, the lateral loads are assumed

to vary linearly from a maximum value at the roof level to zero at the level under consideration, as illustrated in Fig. 2a. A plastic hinge is also assumed to occur at mid-span of the beams to which buckled braces are connected. Although the presence of the zipper column delay the apparition of the beam hinging until brace buckling has extended to a few stories, this assumption is maintained for simplicity. Based on these assumptions, the maximum compression force, C_z , that is obtained in the zipper column at each floor is estimated. A similar procedure is adopted for determining the maximum tension forces, T_z , considering that buckling of the braces initiates at the first floor and progresses upwards, as is illustrated in Fig. 2b. When analyzing the various scenarios for C_z and T_z , the axial loads acting in the beams located above the braces that are on the verge of buckling are also computed and the beams are verified to ensure they can are strong enough to force buckling of their supporting braces, and not the opposite.

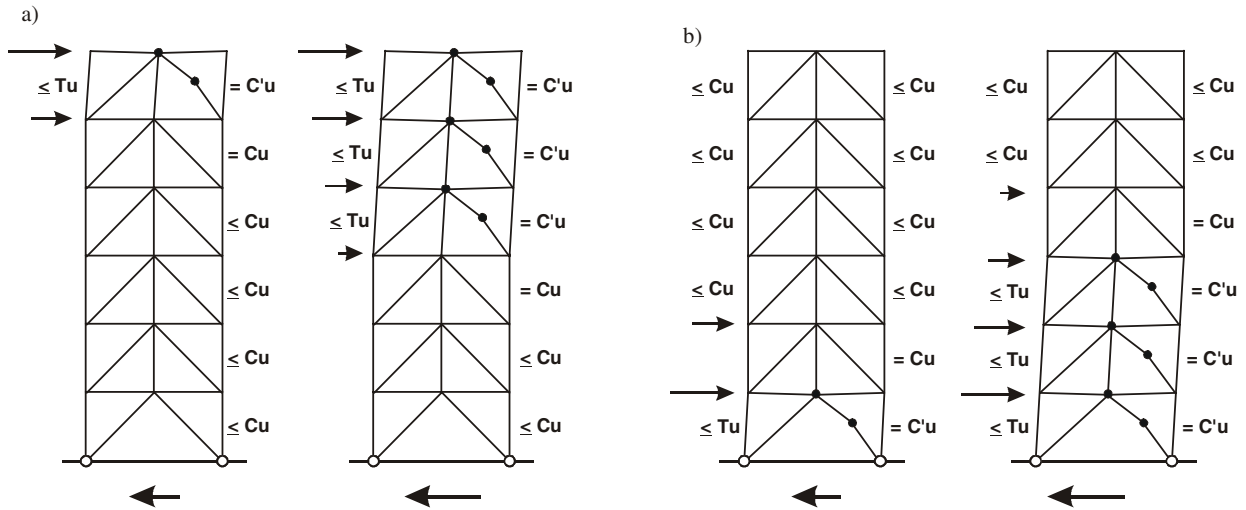


Figure 2: Mechanisms and lateral load distributions adopted for design with brace buckling initiating at the: a) upper floors; b) lower floors.

BUILDINGS STUDIED

Design of the buildings

The design methodology was applied to the N-S bracing bents of the symmetrical a 4-, 8- and 12-storey office building illustrated in Figure 3. The structures were assumed to be located on a firm ground site in Victoria, B.C., Canada. The design was performed according to the upcoming 2005 edition of the National Building Code of Canada [10] and the CSA-S16-01 Standard [3], assuming the frame classifies as a Type MD (Moderately Ductile) braced frame. The gravity dead (D) and live (L) loads at the roof level were equal to 3.4 and 1.48 kPa, respectively. The corresponding loads at the floor levels were 4.5 and 2.4 kPa. The weight of the exterior cladding was taken equal to 1.2 kPa. In NBCC 2005, the minimum design lateral earthquake force, V , is given by:

$$[1] \quad V = \frac{S(T_a) M_V I_E W}{R_d R_o} \leq \frac{2 S(0.2) I_E W}{3 R_d R_o}$$

In this expression, T_a is the fundamental period for design, S is the design spectrum corresponding to a of 2% in 50 years hazard level, M_V is a factor to account higher mode effects on base shear, I_E is the importance factor, W is the seismic weight, and R_d and R_o are respectively the overstrength- and ductility-related force modification factors. Values of S for the site at $T = 0.2, 0.5, 1.0,$ and 2.0 s were respectively

equal to 1.20, 0.83, 0.38, and 0.19 g (Adams et al. [11]). S was obtained by linear interpolation for $T < 2.0$ s and was taken as $S(2.0 \text{ s})$ for T equal to or greater than 2.0 s. For the structures studied, the M_v factor was equal to 1.0 and the buildings were of the normal importance category with $I_E = 1.0$. The force modification factors $R_d = 3.0$ and $R_o = 1.5$ were used in the calculations. Table 1 gives the total seismic weight for the buildings, the design period and corresponding S factor, and the design base shear per frame. Note that accidental in-plane torsion was omitted for simplicity. The load V was distributed over the building height according to the NBCC equivalent static procedure, with a concentrated load at the roof level for higher mode effects, F_t , for the 8- and 12-storey buildings. The load F_t and the computed periods of vibrations in the first two modes of vibrations for the three structures are also given in Table 1, as well as the S factor for the computed period T_1 .

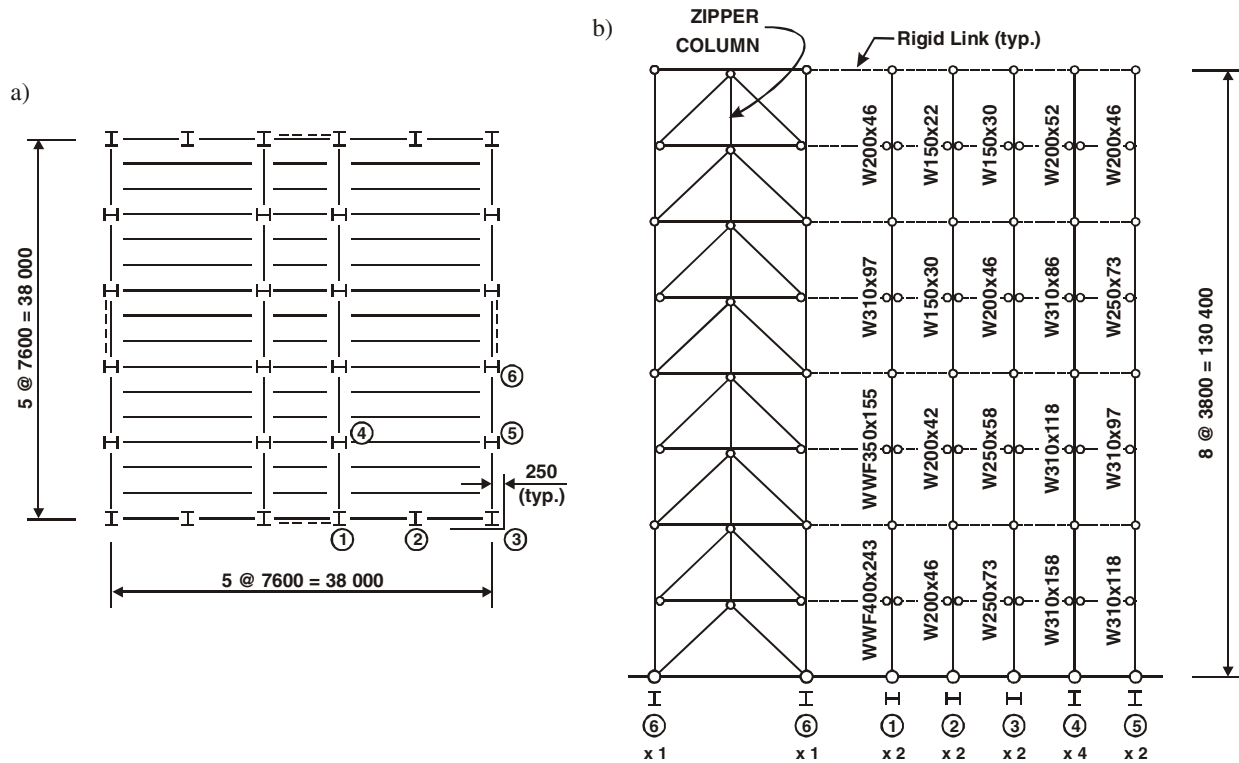


**Figure 3: Building studied: a) Plan view;
b) Elevation of the 8-storey zipper braced frame and tributary gravity columns.**

Table 1 Seismic design and characteristics of the buildings studied

Height (stories)	W / Building (kN)	T_a (s)	$S(T_a)$ (g)	V / Frame (kN)	F_t / Frame (kN)	T_1 (s)	T_2 (s)	$S(T_1)$ (g)
4	28 060	0.58	0.76	2370	-	0.73	0.27	0.62
8	57 550	0.97	0.41	2600	177	1.63	0.56	0.26
12	87 040	1.32	0.32	3100	285	2.66	0.83	0.19

All braces and the zipper columns were made of hot formed, square hollow structural sections, except for the 12-storey building for which W-shapes had to be used for the zipper columns in the lower floors. For all buildings, W shapes were used for the beams and the columns. All members were made of steel with $F_y = 350\text{MPa}$ and an effective length factor of 0.9 was used both for the braces and the zipper columns. The design of the braces was governed by compression resistance and maximum width-to-thickness ratio for

ductile behavior. The zipper columns and the columns were designed to remain elastic under gravity and seismic actions. The envelope of the design zipper column loads in tension and compression are given in Fig. 7, together with the computed peak forces obtained from analysis. The analytical results will be discussed later.

Analytical procedure

Nonlinear time-history dynamic analysis was performed using the Drain-2D computer program by Kanaan and Powell [12]. The numerical model for the 8-storey building is illustrated in Figure 3b. The same model was used for the 4- and 12-storey structures. It included one of the two bracing bents acting in the N-S direction as well as the gravity columns laterally stabilized by that braced frame. The bracing members and the zipper columns were modeled using the inelastic brace buckling element with pinned ends (Element no. 9) developed by Jain & Goel [13]. The brace compressive strength was set equal to C_r/ϕ , with $C_r = \phi A F_y (1 + \lambda^{2n})^{-1/n}$, conforming to the CSA-S16 Standard. The brace post-buckling strength was assumed equal to $C'_u = A F_y (a + b \lambda^c) \leq C_u$ [14]. In these expressions, A is the brace cross-section area, F_y is the yield strength, λ is the brace slenderness parameter, $n = 2.24$ for rectangular hollow section profile and 1.34 for W-shapes, $a = 0.084$, $b = 0.12$, and $c = 1.61$. The slenderness parameter λ was computed as: $\lambda = KL/r (F_y/\pi^{2E})^{0.5}$, where KL/r is the brace effective slenderness with $K = 0.9$ and $E = 200000$ MPa.

The columns were assumed to be continuous over two consecutive stories and zero-moment connection splices were specified. Beams were assumed to be pin-connected to the columns. The beams and the columns were modeled using beam-column elements with elastic-plastic hinges located at the ends and mid-span. A Newmark constant acceleration integration scheme with a time step of 0.0005 s was used in the study. P- Δ effects were included with gravity loads due to D+0.5L combination, and 5% Rayleigh damping was specified in the first two modes of vibration.

Table 2 Characteristics of the scaled earthquake ground motions

No.	Event	Magn	R (km)	Station	Comp	PHA (g)	PHV (m/s)	t_d (s)	Target Scale Factor	t (s)
Regular ground motions										
R1	Simulated Trial #1	M_w 6.5	30	-		0.53	0.57	4.7	1.0	8.53
R2	Simulated Trial #4	M_w 6.5	30	-		0.39	0.31	5.7	1.0	8.53
R3	Simulated Trial #1	M_w 7.2	70	-		0.25	0.30	12.5	1.0	18.18
R4	Simulated Trial #2	M_w 7.2	70	-		0.26	0.24	13.1	1.0	18.18
R5	1984 Morgan Hill	M_s 6.1	38	San Ysidro, Gilroy #6	90°	0.29	0.37	6.5	1.0	60.02
R6	1994 Northridge	M_w 6.7	44	Castaic, Old Ridge	90°	0.57	0.52	9.1	0.8	60.00
R7	1965 Puget Sound	M_w 6.7	87	Olympia, Test Lab	266°	0.20	0.13	20.8	2.0	81.96
R8	1949 Western Wash.	M_w 7.1	76	Olympia, Test Lab	86°	0.28	0.17	18.1	1.4	89.06
Near-fault ground motions										
N1	1995 Kobe	M_w 6.9	0.6	JMA	90°	0.83	1.04	-	0.72	150
N2	1995 Kobe	M_w 6.9	2.0	Takatori	90°	0.61	1.75	-	0.97	40.96
N3	1994 Northridge	M_w 6.7	7.1	Rinaldi	228°	0.84	1.75	-	0.72	14.95
N4	1994 Northridge	M_w 6.7	7.1	Newhall	90°	0.58	1.18	-	1.03	40.00
N5	1994 Northridge	M_w 6.7	9.9	Sylmar County Hospital	90°	0.85	1.38	-	0.69	30.00
N6	1994 Northridge	M_w 6.7	6.4	Sylmar-Converter Station	52°	0.6	1.22		1.00	60.00
Cascadia subduction ground motions										
C1	Simulated Trial #1	M_w 8.5	120±	-	-	0.10	0.17	65.1	2.2	100.0
C2	Simulated Trial #2	M_w 8.5	120±	-	-	0.093	0.24	51.4	2.2	100.0

The structures were subjected to three ensembles of ground motions. The first set included 8 regular ground motions (4 simulated and 4 historical motions) which correspond to the two dominant magnitude-hypocentral distance scenarios for the Victoria region (M6.5 at 30 km and M7.2 at 70 km). The second ensemble is composed of 6 near-fault ground motions and the third subset contains two simulated ground motions simulating a Cascadia subduction scenario. The characteristics of the scaled simulated seismic ground motions for Victoria, used in this study, are presented in Table 2. This table contains presents the magnitude, the hypocentral distance, R, the peak horizontal ground acceleration (PHA) and velocity (PHV), the Trifunac duration, t_d , the target scale factor, and the total duration of the record considered, t. For the regular and subduction time histories, the records were scaled to match the design spectrum (S) over the applicable period range. For the near-fault ground motions subset, the records were scaled such that their peak ground acceleration was equal to 0.60 g, corresponding approximately to the PGA for the site at an annual probability of 2% in 50 years (0.62 g).

PERFORMANCE OF THE BUILDINGS

Overall response

All 4-storey buildings exhibited stable inelastic response under all ground motions. For the 8-storey structures, collapse by dynamic instability was observed under four near field motions and two Cascadia earthquakes. For each of these records, the ground motion amplitude had to be reduced until the structure could withstand the ground shaking. Similarly, for the 12-storey buildings, the amplitude of three near-fault ground motions and one Cascadia subduction records had to be diminished to prevent collapse by instability. For both the 8-storey and 12-storey buildings, Table 3 gives the scale factor, the peak ground acceleration, and the 5% damped spectral amplitude at the building fundamental period T_1 for all records. Shaded cells indicate records with reduced amplitude. Unless otherwise specified, all response parameters presented herein were obtained using these reduced amplitude motions.

Table 3 Characteristics of the records with modified amplitude for the 8- and 12-storey buildings

No.	Time history	8-storey structure			12-storey structure		
		Scale Factor	PHA (g)	Sa (1.63 s)	Scale Factor	PHA (g)	Sa (2.66 s)
R1	Simulated Trial #1	1.0	0.28	0.28	1.0	0.28	0.22
R2	Simulated Trial #4	1.0	0.24	0.24	1.0	0.24	0.12
R3	Simulated Trial #1	1.0	0.32	0.32	1.0	0.32	0.20
R4	Simulated Trial #2	1.0	0.33	0.33	1.0	0.33	0.12
R5	1984 Morgan Hill	1.0	0.22	0.22	1.0	0.22	0.06
R6	1994 Northridge	0.8	0.30	0.30	0.8	0.30	0.09
R7	1965 Puget Sound	2.0	0.23	0.23	2.0	0.23	0.08
R8	1949 Western Wash.	1.4	0.20	0.20	1.4	0.20	0.15
N1	Kobe JMA	0.72	0.60	0.46	0.72	0.60	0.15
N2	Kobe Takatori	0.53	0.32	0.82	0.70	0.43	0.46
N3	Northridge Newhall	1.03	0.60	0.42	1.03	0.60	0.19
N4	Northridge Rinaldi	0.52	0.44	0.62	0.60	0.50	0.23
N5	Northridge Sylmar H	0.61	0.52	0.57	0.68	0.58	0.34
N6	Northridge Sylmar C	0.99	0.59	0.57	1.00	0.60	0.34
C1	Simulated Trial #1	1.36	0.14	0.23	1.77	0.18	0.16
C2	Simulated Trial #2	1.97	0.18	0.29	2.20	0.22	0.19

The $S(T_a)$ factors used in the design of the 8- and 12-storey structures (0.41 and 0.32 g in Table 3) exceed the spectral ordinates at $T = T_1$ for all regular ground motions in Table 3. No instability was observed for these motions. Conversely, the spectrum values from near field events are larger than the design values for all cases but one for which instability occurred. For the Kobe JMA and Newhall near-fault records, the

ground motion spectral ordinate is close to, or lower than the design values. This suggests that such ground motions can impose relatively higher demand on structures, even when scaled to the peak ground acceleration anticipated for the site. For the subduction earthquake records, the amplitude of the motions had to be reduced even if the ground motion spectral values at the target scale factors were lower than the design values. Past studies (e.g., [15]) have shown that such long duration records can lead to significantly higher displacement demand compared to regular motion.

The mean + one standard deviation (Mean+SD) and maximum values of the peak inter-storey drifts for each ground motion ensemble are presented in Fig. 4 for all three buildings. Under the regular motions, the performance is satisfactory as with mean+SD storey drifts within the code limit of $2.5\% h_s$. The maximum storey drifts among all ordinary motions only slightly exceeded the code limit at some locations along the height of the 4- and 8-storey structures. The near-fault motions induced storey drift angles in excess of the 2.5% limit. The maximum deformations under the Cascadia ground motions remained below the code limit. For the regular and Cascadia ground motions, there was no significant tendency to damage concentration at specified levels, demonstrating the efficiency of the zipper columns in achieving more uniform storey drift distribution over the structure height.

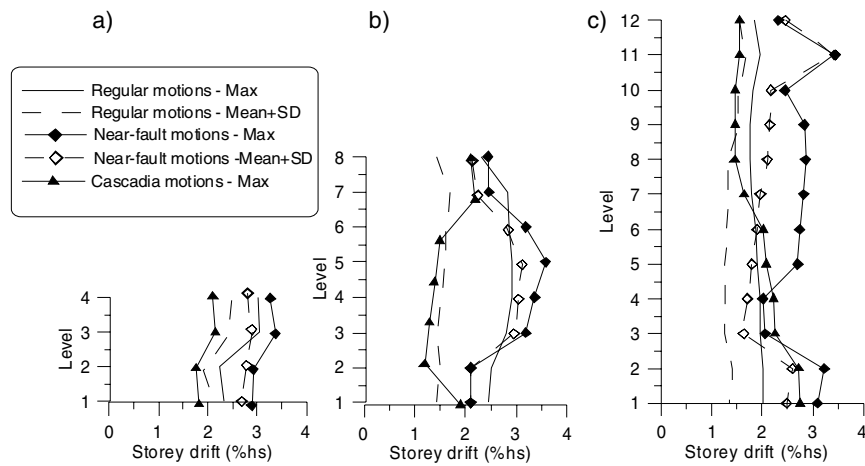


Figure 4: Computed peak storey drifts for the: a) 4-storey building; b) 8-storey building; and c) 12-storey building.

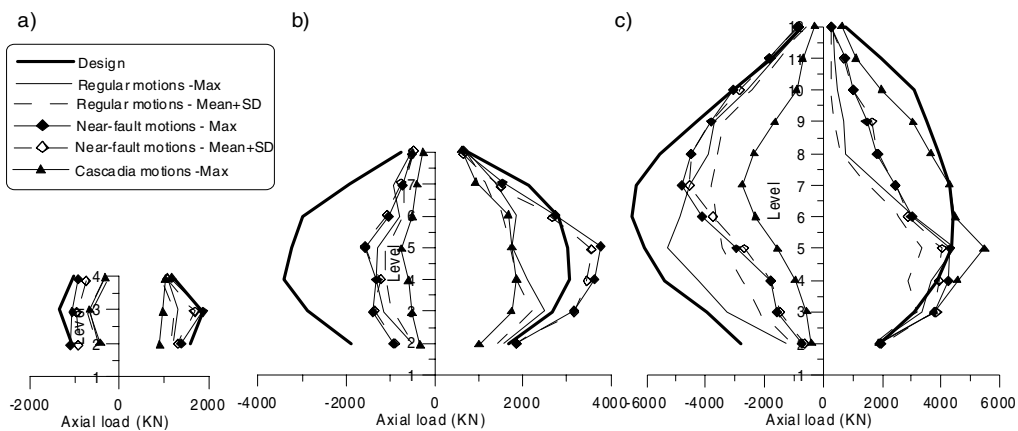


Figure 5: Computed peak axial loads in zipper columns for the: a) 4-storey building; b) 8-storey building; and c) 12-storey building.

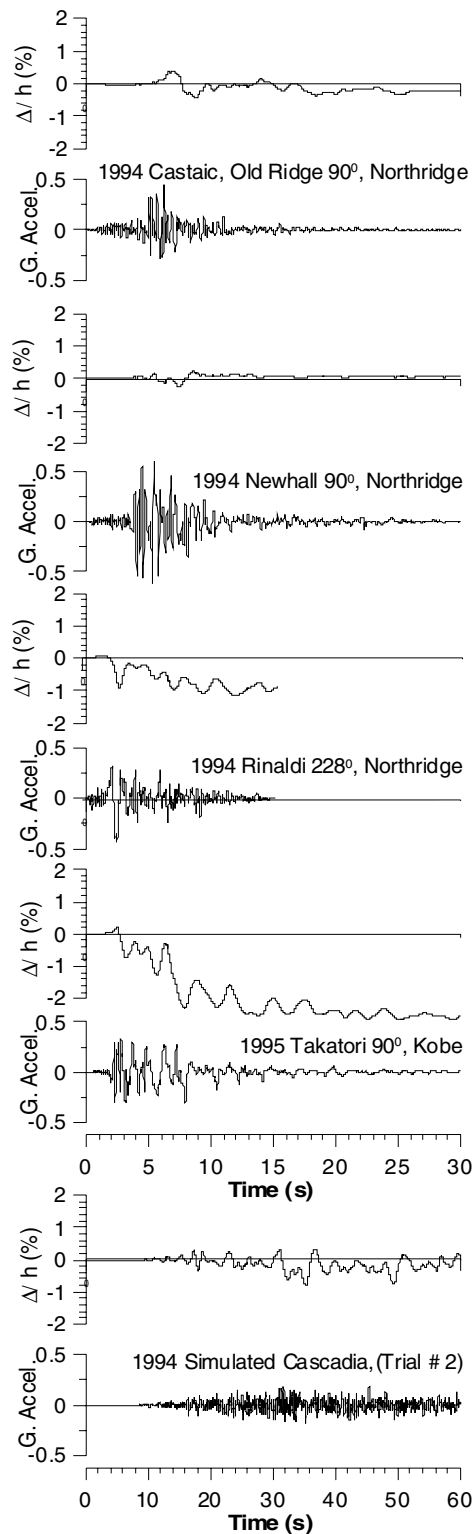


Figure 6: Ground motion and roof displacement time histories for Records R6, N3, N4, N2, and C1.

Figure 5 presents the statistics of the peak zipper column loads for all buildings under all ground motion subsets. Under the regular and subduction ground motions, the computed peak zipper columns loads remained below the design forces for the 4- and 8-storey structures. For the 12-storey buildings, the design tension loads was slightly exceeded at the 3rd floor under motion R2 (8%) and at the 5th floor under motion R3 (3%). For the 8-storey structures, the predicted zipper column load was exceeded at a PGA of 0.35g for the Rinaldi motion, 0.60 g for the NewHall record, and 0.40 g for the two Sylmar records. For the 12-storey building, the design tension loads were exceeded at the 3rd floor under all near field motions (by 3 to 20%) and at the 4th floor under the Newhall motion (by 10%). Similarly, the tension forces that developed in the zipper column at Levels 3 to 5 exceeded the design predicted values under the Cascadia subduction motions. The design compression load was exceeded at the 11th and 12th floors under the Kobe JMA record (by 3%) and at the 11th (3%) and 12th (14%) floors under the Newhall record. In all these cases, the zipper column remained elastic, however, due to reserve capacity exhibited by the column members (use of material resistance factors in design, limited choices of available sections and, when tension loads were excessive, because the design was governed by compression).

Detailed response analysis

Close examination of the building response revealed that buckling of the braces initiated either at the base of the building or at the top floor, as assumed in the design procedure that was used for the zipper column. For the 4-storey building, the peak axial compression and tension forces computed in the zipper column were lower than those predicted by the proposed method. The largest forces were induced by the near-fault motion ensemble. Under the regular motion R6, brace buckling initiated at the 3rd floor and then propagated towards the base (Fig. 7a). Upon load reversal, buckling initiated at the first floor on the other side of the frame and then rapidly propagated towards the top floor. For all other regular motions, brace buckling started at the base and then developed nearly simultaneously in the upper stories.

Under near-field motions, the first brace buckled at the base and buckling then propagated towards the top of the structure, as shown in Fig. 7b for motion N6. In this example, after the motion was reversed ($t = 4.14s$), buckling of the braces developed from the base to the top within 0.16 s. This behavior resulted in large axial tension force in the zipper column, starting in the lower levels and migrating towards the top. The same response was observed for all near-field motions.

Under the Cascadia subduction motion C1, brace buckling also started at the base at $t = 14.0$ s but the amplitude of the shaking was not sufficient buckling over the building height, as shown in Fig. 7c. Upon load reversal, brace buckling then developed over the four stories.

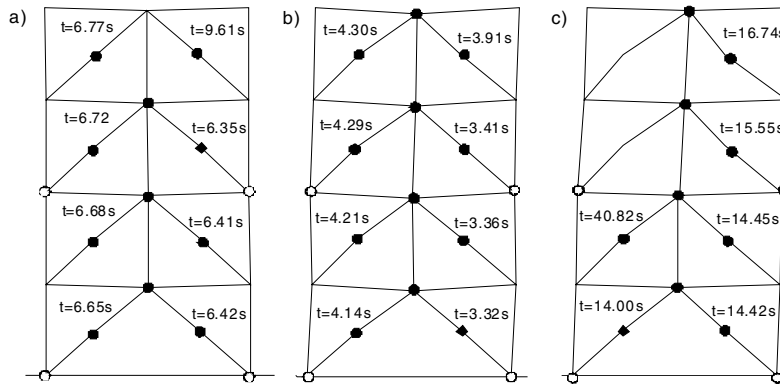


Figure 7 Sequence of brace buckling and beam hinging for the 4-storey building under:
a) Regular motion R6; b) Near-fault motion N6; c) Cascadia simulated motion C1
(♦ First brace buckling; • Subsequent brace buckling and hinging).

For the 8-storey building, the response under ordinary motions was satisfactory with storey drifts remaining within the code limit. For all motions except record R2, brace buckling started at the base and developed upwards. Under motion R2 (Fig. 8a), the first brace buckled at the 8th level but the next occurrence of buckling was at the base in both directions of oscillation. Figure 10a shows the time history of the response at three levels under record R6. The maximum peak storey drift under that motion was 1.5% h_s at the 6th level. The response is symmetrical and harmonic in nature with no large permanent drifts developing in one direction. The vertical distribution of the lateral loads and the zipper column loads are shown at two different times on the right-hand side of the figure. The design lateral load scenarios and design zipper column loads are also shown in the figure for comparison. The largest tension zipper column load developed at $t = 7.63$ s at the 3rd floor, which agrees well with the prediction. At 9.56 s, the largest storey drift developed at the 8th floor and the maximum lateral load at the roof level at that time is below the prediction.

The Mean+SD storey drift values are generally beyond the code limit under the near-fault ground motions. In particular, the Kobe Takatori record contributed significantly to the deformation pattern with the large amplitudes at the intermediate floors shown in Fig. 4b, both the maximum and the Mean+SD values plotted (up to 3.6% at the 5th floor and large values at levels 4 and 6). For the other near field motions, the maximum drifts over the height reached approximately 2.5% h_s . Due to the large amount of energy input by these near field motion, full mechanisms developed on both sides of the frame within single half-cycle excursions, starting from the base, as illustrated in Fig. 8b. Differences could be noted, however, between the near-fault records, as illustrated in Fig. 6 showing ground motion and corresponding computed roof displacement time histories for selected ground motions. The Northridge Newhall record is characterized by several acceleration pulses with short duration that produced very limited roof displacements. The Northridge Rinaldi record contains one long acceleration pulse that produced a large movement at the roof level. In the Kobe Takatori record, several successive large pulses resulted in significant cyclic response with displacements gradually increasing towards one direction (crawling or ratcheting effect).

Figure 10 show storey drift time histories of the 8-storey building under the Rinaldi and Takatori records. The residual deformation pattern is also given for the cases as well as lateral loads and zipper column axial forces at two different times during these motions. Under the Rinaldi motion, the whole building moved towards one direction during the beginning of the acceleration pulse. Upon load reversal, only the first two floors reversed direction while the rest of the structure remained on one side, especially the intermediate part of the structure (levels 3-4), while the upper floors tried to move back to return to the undeformed position. First mode response developed under the Takatori record up to the large pulse at $t = 5.5$ s where stories 1 and 2 moved towards one direction while stories 3 to 5 deformed in the opposite direction, resulting in the S-shape mechanism that remained until the end. Under the Rinaldi record, large lateral loads developed at the bottom of the structure while the loads remained very small in the upper floors. At the beginning of the pulse ($t = 2.38$ s), the load pattern was similar to what was assumed in design but the zipper load was slightly exceeded. Later, a force larger than anticipated was observed at Level 4, with nearly zero force at Level 1, which was different than assumed in design and resulted in higher zipper tension load in the zipper column. The lateral load patterns illustrated for the Takatori motion are similar to those observed under the Rinaldi record but the amplitudes are lower and the values of C_z remained with the predictions. It is interesting to note that the Takatori record produced lateral loads acting in opposite directions.

For the two Cascadia motions, brace buckling started at the base of the 8-storey building and the response was more important at the bottom and top floors with smaller storey drift values in the middle region of the structure. Collapse under these ground motions when scaled to the target scale factor can be attributed to the long duration of strong motion exhibited by the records. This resulted in several reversals of inelastic loading that concentrated in the lower floors. The braces gradually lost their compressive resistance, pinching became more pronounced, and large deformations and beam plastic hinges developed in the two bottom stories. Zipper column loads were transferred to the outer columns. A single-storey mechanism eventually formed at the bottom floor with plastic hinging forming in the first column tier.

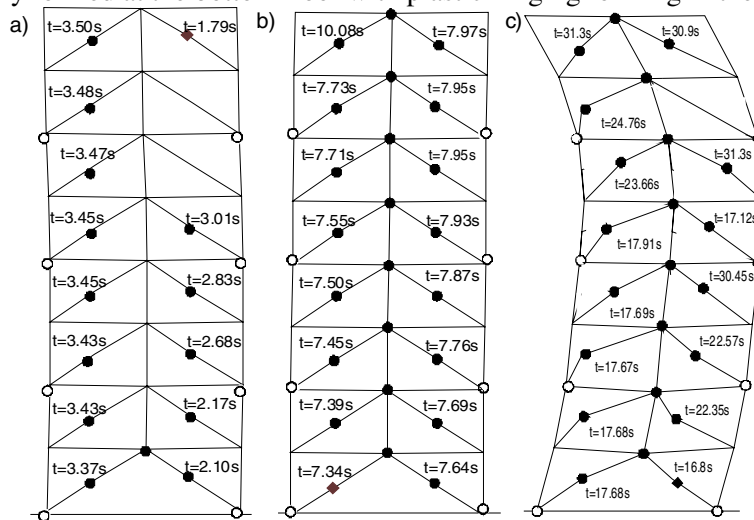


Figure 8: Sequence of brace buckling and beam hinging for the 8-storey building under:
a) Regular motion R2; b) Near-fault motion N1; c) Cascadia motion C2
(♦ First brace buckling; • Subsequent brace buckling and hinging).

For the 12-storey building, the inter-storey drift demand under the regular motion ensemble is equally distributed over the structure height and the maximum values are below the code limitation. Axial compression forces in the zipper columns exceeded the tension forces under the regular and near-fault motions, which was not the case for the 4- and 8-storey structures. However, the computed compression load envelop matches the design zipper column loads. Examining the frame responses, it is found that for

six of the regular motions and two of the near-field motions, buckling of the braces initiated in the top part of the building, which resulted in the large zipper compression loads in the topmost floors. For instance, buckling initiated at the uppermost floor under the regular motion R8 (Fig. 9a), propagated towards the middle floors to eventually develop in the lower half of the structure. After the earthquake reversed sign and $t = 7.8$ s, brace buckling was initiated at the top floor on the other side to propagate simultaneously over nearly the whole building height. The largest axial compression forces in the zipper columns are associated to this case. This high demand in the top part of the structure is attributed to higher mode response, as was anticipated in the proposed procedure for predicting zipper compression loads. When several braces buckle in the upper part of the structure, as this is the case under motion R8 (Fig. 9a), the zipper column is no longer “supported” by the elastic braces located in the upper portion of the structure, preventing large tension forces to develop in the zipper column when buckling develops later in the lower part of the building. This behavior was not observed for the 4- and 8-storey buildings for which higher mode response was less pronounced and brace buckling started at the base. For the 8-storey frame under the R2 motion, the first buckling occurrence was observed at the top of the structure but buckling did not extend towards the base, thus allowing tension zipper loads to develop at a later time during the earthquake.

In Fig. 6, the roof displacements under the Newhall record are small, indicating significant higher mode response, likely due to the relatively high frequency of the motion. For this earthquake, large lateral loads developed at the roof level, as can be seen in Fig. 10, and brace buckling started at the top floor. For other motions with longer acceleration pulses and higher energy input, such as the Takatori and Rinaldi records, brace buckling initiated at the base and propagated towards the top, as shown in Fig. 9b. Under the near-fault motion N3, the first brace buckled at the base and all braces then buckled simultaneously towards the top as a result of the large impulse. On the other side of the frame, only the braces in the upper part buckled later. This response produced large tension forces and small compression forces at the base of the zipper column. The development of brace buckling for the 12-storey structure subjected to Cascadia motions was similar to that observed under motion N3, as illustrated in Fig. 9c. Fig. 10 shows snap shots of the lateral load and zipper column load distributions under the Newhall record. As indicated, large concentrated lateral loads developed at individual floors in the building, which is different than the triangular shapes assumed in design. That situation was also observed for the subduction motions, which resulted in zipper tension loads in excess of the predictions.

This difference in behavior demonstrates that the force pattern in the zipper columns strongly depends on the location of the first occurrence of brace buckling. When brace buckling initiates in the upper levels, large compression forces develop in the top part of the zipper column and tension loads in that zone are limited by the post-buckling strength of the braces (and the flexural capacity of the beams) in the upper levels. When buckling starts at the base, large tension loads develop in the zipper columns at the bottom levels and the zipper column is no longer vertically supported by the lower storey braces such that no large compression force can develop in the lower portion of the building. If buckling propagates from the top towards the base over a significant portion of building height, the tension forces will be limited in the zipper column over the entire height of the structures. Similarly, when buckling propagates from the base up to the roof, very limited compression is observed in the zipper columns. Therefore, tension will be dominant for low-rise structures which respond mainly in their first mode whereas for taller frames, for which higher mode response is more important, compression is likely to concentrate in the upper part and tension at the base of the structure. The relative amplitude of these two forces will depend on the development of brace buckling in the structure. For some structures and some ground motions, tension will dominate whereas compression can be larger in others situations. For instance, under the Newhall record (see Fig. 10), large tension forces were observed at the base although brace buckling started at the top level.

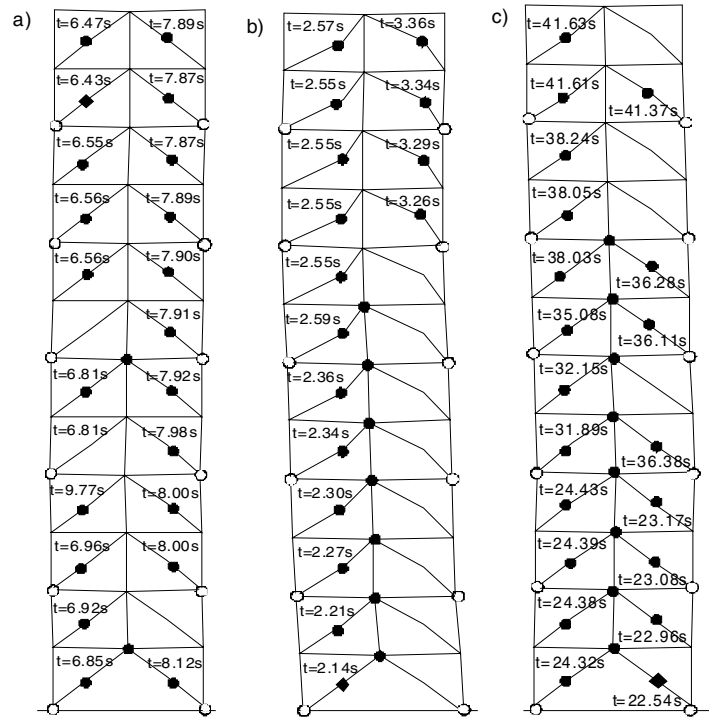


Figure 9: Sequence of brace buckling and beam hinging for the 12-storey building under:
a) Regular motion R8; b) Near-fault motion N3; c) Cascadia motion C2
(♦ First brace buckling; • Subsequent brace buckling and hinging).

CONCLUSIONS

An analytical study was carried out to examine the influence of the building height and the ground motion type on the seismic performance of zipper concentrically braced steel frames. Analyses were performed on 4-, 8-, and 12-storey building structures subjected to three different ground motion ensembles: ordinary ground motions from crustal and sub-crustal events, records from near-field earthquakes, and long duration ground motions produced by subduction events. The design axial loads for the zipper columns were determined with the method proposed by Tremblay and Tirca [8].

All structures behaved as anticipated in terms of the sequence of brace buckling, i.e. with buckling of the braces initiating either at the top or at the base of the structures and then propagating along the building height to a degree that varied with the building height and the ground motion characteristics. Maximum compression forces in the zipper columns resulted from buckling of the upper floor braces, which occurred due to higher mode response such as in taller frames or when the ground motion dominant period was shorter than that of the structures. Conversely, the largest tension loads in the zipper columns developed at the lower levels as a result of first mode response (lower frames) or when the structure was hit by motions that included long duration acceleration pulses. Peak zipper column loads from analysis agreed well with the predicted values except that the forces obtained from analysis exceeded the design values for some ground motions in the lower part of the 8- and 12-storey structures (by 3-20%) and at the top two floors of the 12-storey structures (by 3-14%). Yielding and buckling did not occur, however, due to the reserve capacity of the zipper columns. The analyses indicated that additional loading scenarios such as lateral loads applied at individual stories in the lower half of the buildings should permit to overcome this situation. Further study is needed to validate this assumption.

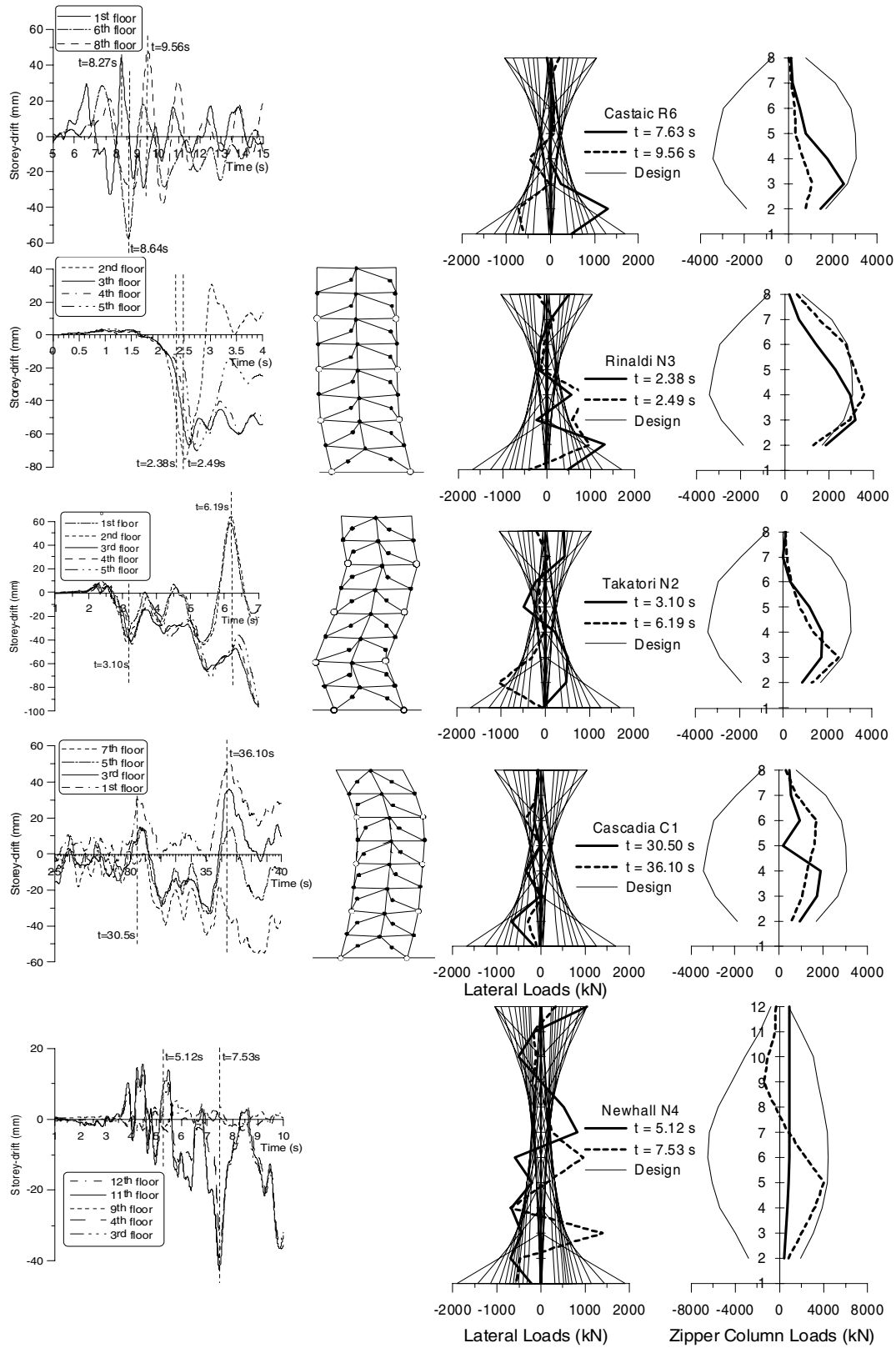


Figure 10: Detail of response of the 8-storey building under record R6, N3, N2, and C1, and of the 12-storey building under Record N4.

Stable inelastic response, with storey drifts within the applicable limit, was obtained for all structures when subjected to ordinary ground motions. Under near-fault and Cascadia motions, the study indicated that collapse by dynamic instability is a possibility for the 8- and 12-storey structures, even if the zipper columns remained elastic. Such instability is attributed in to the poor brace hysteretic response, the large demand at long period for the near field records, and the long duration of shaking for the subduction earthquakes. This is contrary to earlier expectations that zipper braced frames would not be sensitive to the signature of the ground motions. Therefore, zipper systems are not recommended for structures taller than 4 stories exposed to near-field or subduction seismic conditions unless stable inelastic response can be demonstrated. It is recommended that further studies including incremental dynamic analysis be conducted to better evaluate the seismic performance of tall zipper frames.

ACKNOWLEDGEMENTS

This research was supported by the Natural Sciences and Engineering Research Council of Canada and the Fonds pour la nature et les sciences of the Government of Quebec.

REFERENCES

1. Khatib, I.F., Mahin, S.A., and Pister, K.S. *Seismic Behavior of Concentrically Braced Steel Frames*. Report UCB/EERC-88/01, Earthquake Engineering Research Center, Univ. of California, Berkeley, CA, 1988.
2. Tremblay, R. and Robert N. "Seismic Performance of Low- and Medium-Rise Chevron Braced Steel Frames." *Can. J. of Civ. Eng.* 2001; 28(4): 699-714.
3. CSA. "Limit states design of steel structures, CSA-S16-01." Canadian Standards Association, Rexdale, ON, 2001.
4. Remennikov, A.M. and Walpole, W.R. "Seismic Behavior and Deterministic Design Procedures for Steel V-Braced Frames." *Earthquake Spectra* 1998; 14(2): 335-355.
5. Sabelli, R. "Research on Improving the Design and Analysis of Earthquake-Resistant Steel-Braced Frames." NEHRP Fellowship Report No. PF2000-9, Earthquake Engineering Research Institute, Oakland, CA, 2001.
6. AISC. "Seismic Provisions for Structural Steel Buildings - ANSI-AISC 34102." American Institute of Steel Construction, Chicago, IL, 2002.
7. ECS. "Eurocode 8: Design of structures for earthquake resistance, May 2001 Draft." European Committee for Standardization, Brussels, 1998.
8. Tremblay, R. and Tirca, L. "Behaviour and design of multi-storey zipper concentrically braced steel frames for the mitigation of soft-storey response." In F. Mazzolani (eds.), *Behaviour of Steel Structures in Seismic Area; Proc. STESSA 2003 Conf.*, 471-478, Naples, Italy, June 2003. Rotterdam: Balkema.
9. Tremblay, R. "Achieving a Stable Inelastic Seismic Response for Concentrically Braced Steel Frames." *Eng. J.*, AISC 2003; 40(2): 111-129
10. NRCC. "Proposed changes to NBC 1995 – Part 4. National Research Council of Canada." Institute for Research In Construction. Ottawa, ON, Canada, 2001.
11. Adams, J., Weichert, D. H., and Halchuk, S. "Trial Seismic Hazard Maps of Canada – 1999: 2%/50 Year Values for Selected Canadian Cities." Geological Survey of Canada Open File 3274, National Earthquake Hazards Program, Geological Survey of Canada, Natural Resources Canada, Ottawa, ON, 1999.
12. Kanaan A.E., Powell G.H. "DRAIN-2D. *Report Nos. EERC 73-6 and 73-22* (revised in 1975)." Earthquake Engineering Research Center, Univ. of California, Berkeley, CA, 1978.
13. Jain, A.K. and Goel, S.C. "Hysteresis Models for Steel Members Subjected to Cyclic Buckling or Cyclic End Moments and Buckling (User's Guide for Drain-2D: EL9 and EL10). *Report UMEE 78R6*, Dept. of Civ. Eng., Univ. of Michigan, Ann Arbor, MI, 1978.
14. Tremblay, R. "Inelastic Seismic Response of Bracing Members. *J. of Const. Steel Research* 2002; 58: 665-701.
15. Tremblay, R. "Development of Design Spectra for Long Duration Ground Motions from Cascadia Subduction Earthquakes." *Can. J. of Civ. Eng.* 1998; 25: 1078-1090.